Solid-State Electronics 199 (2023) 108491

Contents lists available at ScienceDirect

Solid State Electronics

journal homepage: www.elsevier.com/locate/sse

Comprehensive evaluation of torques in ultra-scaled MRAM devices ☆

S. Fiorentini [a,b,*], J. Ender [a,b], S. Selberherr [b], R.L. de Orio [b], W. Goes [c], V. Sverdlov [a]

[a] Christian Doppler Laboratory for Nonvolatile Magnetoresistive Memory and Logic at the Institute for Microelectronics, Austria
[b] Institute for Microelectronics, TU Wien, Gußhausstraße 27–29/E360, 1040 Vienna, Austria
[c] Silvaco Europe Ltd., Cambridge, United Kingdom

ARTICLE INFO

Keywords:
Spin and charge drift-diffusion
Spin-transfer torque
Magnetic tunnel junctions
STT-MRAM

ABSTRACT

We present a generalization of the coupled spin-charge drift-diffusion formalism capable of accurately describing the spin and charge transport properties through magnetic tunnel junctions. Correction terms enable reproducing oscillations of the spin current in ferromagnets typical for quasi-ballistic transport. Our approach proves necessary to accurately capture an interplay between the interfacial Slonczewski and bulk-like Zhang-Li contributions to the torque in ultra-scaled MRAM devices.

1. Introduction

The introduction of nonvolatility represents a possible solution to the increase in power consumption encountered with the scaling of DRAM and SRAM. Emerging nonvolatile spin-transfer torque (STT) magnetoresistive random access memory (MRAM) offers high speed and endurance, being attractive for stand-alone, embedded automotive, and Internet of Things applications, and for its possible employment in frame buffer memory and slow SRAM [1–5]. The basic component of an STT-MRAM cell is a Magnetic Tunnel Junction (MTJ), composed of two ferromagnetic (FM) layers separated by an insulating tunnel barrier (TB). The magnetization of the Reference Layer (RL) is fixed, while the one of the Free Layer (FL) can be switched. Due to the Tunneling Magnetoresistance (TMR) effect, the resistance of the structure is different, when the magnetization vectors are parallel (P) or anti-parallel (AP) to each other, providing a way of discerning the bit state. The writing process in STT-MRAM is achieved by passing an electric current through the structure. Electrons flowing from the RL to the FL become spin polarized, and the generated spin current is absorbed by the FL, providing the torque [6]. In recently demonstrated ultra-scaled MRAM devices, elongated composite free layers with multiple MgO barriers are employed to boost both the shape- and interface-induced perpendicular magnetic anisotropy [7]. Therefore, when simulating ultra-scaled STT-MRAM, it is paramount to compute all torque contributions, like the interfacial Slonczewski [6] and bulk Zhang-Li [8] torques, from the same source, namely the spin accumulation, in order to capture possible interactions between them.

2. Model

The torque acting on the magnetization can be derived by computing the spin accumulation $\mathbf{S}$ in the whole structure. This allows to obtain both contributions, and their interaction, from the same set of equations. This requirement is achieved by employing the spin drift-diffusion approach for the computation of $\mathbf{S}$ [9,10] with the equations

$$\overline{\mathbf{J_S}} = -\frac{\mu_B}{e}\beta_\sigma \mathbf{m} \otimes \left(\mathbf{J_C} - \beta_D D_e \frac{e}{\mu_B} \left[(\nabla \mathbf{S})^T \mathbf{m} \right] \right) - D_e \nabla \mathbf{S}\,, \tag{1a}$$

$$-\nabla \cdot \overline{\mathbf{J_S}} - D_e \frac{\mathbf{S}}{\lambda_{sf}^2} - \mathbf{T_S} = \mathbf{0}\,, \tag{1b}$$

$$\mathbf{T_S} = -\frac{D_e}{\lambda_J^2}\mathbf{m} \times \mathbf{S} - \frac{D_e}{\lambda_\varphi^2}\mathbf{m} \times (\mathbf{m} \times \mathbf{S})\,, \tag{1c}$$

where μ_B is the Bohr magneton, e is the electron charge, β_σ and β_D are polarization parameters, D_e is the electron diffusion coefficient, λ_{sf} is the spin-flip length, λ_J is the exchange length, λ_φ is the spin dephasing length, $\mathbf{J_C}$ is the charge current density, $\overline{\mathbf{J_S}}$ is the spin current density tensor, $\mathbf{T_S}$ is the spin torque, and $\mathbf{m}$ is the unit magnetization vector. As this formalism only accounts for diffusive and scattering effects, it must be extended to accurately describe the torques acting in an MTJ.

The charge current is modeled by employing a low conductivity which locally depends on the relative magnetization vector's orientation across the tunnel layer [11]. For the spin current, the diffusion coefficient in the TB is set low, proportionally to the conductivity due to the Einstein relation, and the following boundary condition is imposed

☆ The review of this paper was arranged by Francisco Gamiz.

* Corresponding author at: Institute for Microelectronics, TU Wien, Gußhausstraße 27–29/E360, 1040 Vienna, Austria.
E-mail address: fiorentini@iue.tuwien.ac.at (S. Fiorentini).

https://doi.org/10.1016/j.sse.2022.108491

Available online 28 October 2022

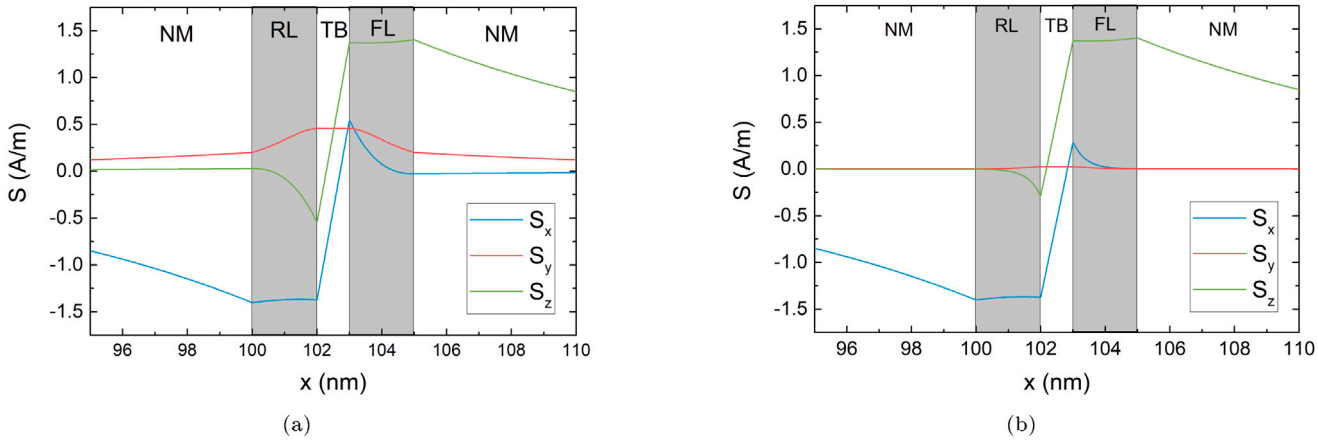

Fig. 1. Spin accumulation in a symmetric MTJ structure. Nonmagnetic contacts are present to let **S** decay. The presence of the TB creates a jump in the **S** components. (a) Results for $\lambda_\varphi = 2$ nm. (b) Results for $\lambda_\varphi = 0.4$ nm.

Table 1
Parameters used in the simulations.

Parameter	Value
Charge polarization, β_σ	0.7
Spin polarization, β_D	0.8
NM diffusion coefficient, $D_{e,NM}$	10^{-2} m^2/s
FM diffusion coefficient, $D_{e,FM}$	2.0×10^{-3} m^2/s
TB diffusion coefficient, $D_{e,TB}$	2.0×10^{-8} m^2/s
NM conductivity, σ_{NM}	5.0×10^{6} S/m
FM conductivity, σ_{FM}	1.0×10^{6} S/m
TB conductivity, σ_0	29.76 S/m
Polarization factors, P_{RL}=P_{FL}	0.707

on the left and right interfaces of the TB:

$$\overline{\mathbf{J_S}} \cdot \mathbf{n} = -\frac{\mu_B}{e} \frac{J_C}{1 + P_{RL}\, P_{FL}\, \cos\theta} [\, P_{RL}\, \mathbf{m_{RL}} + P_{FL}\, \mathbf{m_{FL}}] \tag{2}$$

Here, the subscript RL(FL) indicates the reference (free) layer, P is the Slonczewski polarization parameter [6], J_C is the charge current component orthogonal to the TB, and θ is the local angle between the magnetization vectors in the RL and FL. Thereby, we can reproduce the spin current value [12] when $\mathbf{J_C}$ flows through the TB. The finite element solver discussed in [11] was augmented with the boundary condition (2) in order to produce the results presented in this work. The spin accumulation **S** can be computed from (1b), and the torque is then obtained from (1c).

3. Results

While employing (2) gives the opportunity to fix the spin current density in the TB to the value expected in MTJs, the length parameters entering (1) determine the scale of absorption of the transverse spin accumulation components and the behavior of the torque in the bulk of the FM layers. Fig. 1(a) shows the spin accumulation obtained in a symmetrical MTJ structure with $\lambda_J = 1$ nm, $\lambda_\varphi = 2$ nm, and $\lambda_{sf} = 10$ nm, where the FM layers are 2 nm thick, the TB is 1 nm thick, and two non-magnetic contacts (NM) of 50 nm thickness are included to allow the spin accumulation to decay to zero. The remaining parameters are listed in Table 1. The magnetization points towards x in the RL and towards z in the FL. In this case, the transverse spin accumulation components are not completely absorbed in the FL, contrary to what is usually expected in strong ferromagnets [6,13,14]. By taking an effective dephasing length of $\lambda_\varphi = 0.4$ nm, it is possible to have a faster decay of the transverse components close to the TB interface, cf. Fig. 1(b). The direct proportionality of the STT torque on the sine of the angle between the magnetization vectors in the FM layers predicted in MTJs under a constant voltage [6,12] is reproduced exactly. A comparison with the values obtained using the Slonczewski expression from [6] is shown in Fig. 2.

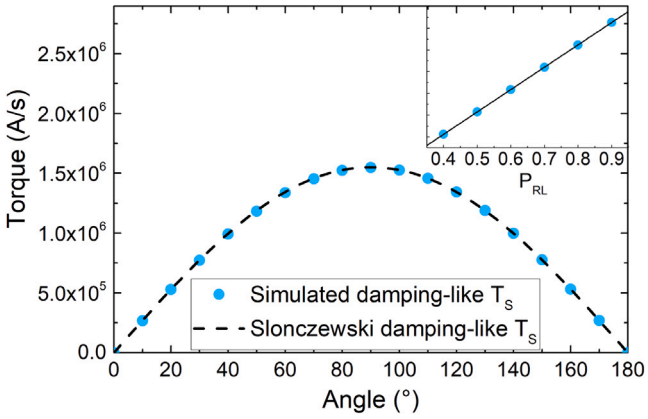

Fig. 2. Dependence of the average torque on the relative angle between the magnetization vectors. The inset shows the linear dependence of the torque on the RL polarization factor.

Recent analytical investigations of the behavior of the torque in the ballistic regime predict a more complex absorption pattern for the transverse components, with an oscillating behavior [12]. By introducing a ballistic correction [15] to the spin drift-diffusion formulation, the complex oscillating behavior of the torque can be reproduced. The additional terms can be derived from the continuous random matrix theory, and stem from the underlying ballistic origin of the transverse spin precession or absorption [16]. The expression for the spin current with the ballistic terms, $\overline{\mathbf{J_{S,bal}}}$, is related to the one in (1a) by

$$\overline{\mathbf{J_{S,bal}}} = \overline{\mathbf{A^{-1}(m)}}\,\overline{\mathbf{J_S}}\,, \tag{3}$$

where $\overline{\mathbf{A(m)}}$ is a magnetization dependent tensor, with the components

$$\overline{\mathbf{A(m)}} = \bar{\mathbf{I}} + \left(\frac{\lambda}{\lambda_J}\right)^2 \overline{\mathbf{A_1(m)}} + \left(\frac{\lambda}{\lambda_\varphi}\right)^2 \overline{\mathbf{A_2(m)}} \tag{4a}$$

$$\overline{\mathbf{A_1(m)}} = \begin{pmatrix} 0 & m_z & -m_y \\ -m_z & 0 & m_x \\ m_y & -m_x & 0 \end{pmatrix} \tag{4b}$$

$$\overline{\mathbf{A_2(m)}} = \begin{pmatrix} m_y^2 + m_z^2 & -m_x m_y & -m_x m_z \\ -m_x m_y & m_x^2 + m_z^2 & -m_y m_z \\ -m_x m_z & -m_y m_z & m_x^2 + m_y^2 \end{pmatrix}, \tag{4c}$$

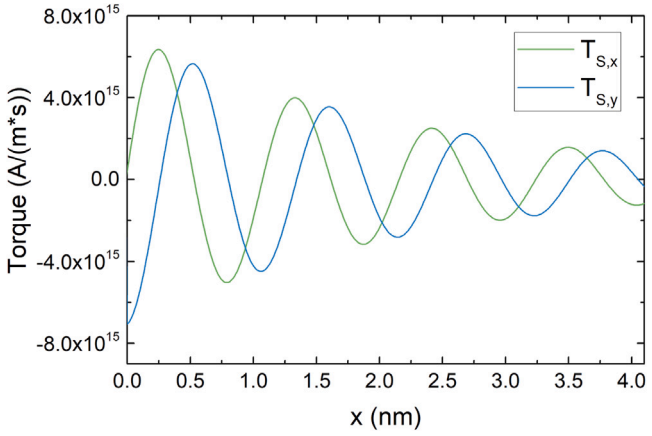

Fig. 3. Torque computed with the inclusion of ballistic corrections to the spin current in a semi-infinite FL. The magnetization configuration is the same one employed for Fig. 1.

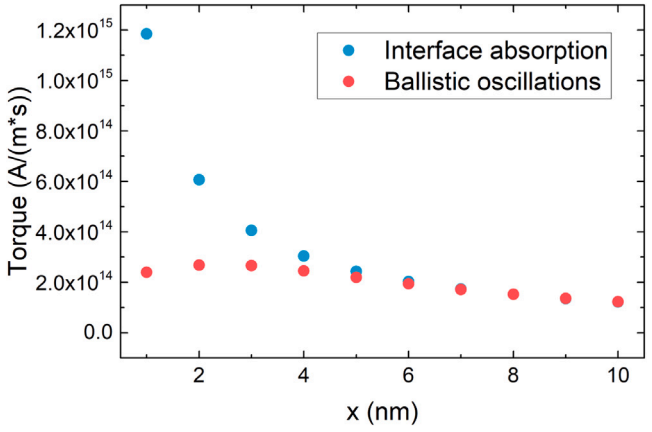

Fig. 4. Comparison of the thickness dependence of the total damping-like torque acting on the FL in the presence of fast interface absorption or ballistic and oscillating behavior of the transverse spin accumulation components.

where λ is the electron mean free path. Eq. (1b) with the spin current described by (3) can be analytically solved. The results for the torque obtained using $\lambda_J = 1$ nm, $\lambda_\varphi = 4.3$ nm, and the mean free path $\lambda = 5.8$ nm in a semi-infinite free layer are shown in Fig. 3. The oscillating behavior of the torque components is in qualitative agreement with the results reported in [12].

The presence of such a pattern has an effect on the total torque exerted on the FL, defined as

$$\mathbf{T}_{\mathbf{S,tot}} = \frac{1}{d_{FL}} \int_0^{d_{FL}} \mathbf{T}_{\mathbf{S}} dx\,, \tag{5}$$

where d_{FL} is the total length of the FL and $\mathbf{T_S}$ is defined by (1c). In Fig. 4, a comparison of the dependence of the total damping-like torque computed with both (1a) and (3) is depicted. For long FLs, both approaches show a $1/d_{FL}$ decay of the total exerted torque. Below 4 nm, however, the transverse components are not completely absorbed in the ballistic approach, so that the dependence of the torque on the FL thickness becomes more complex, and its value is reduced. Such a difference in the thickness dependence of the torque can provide a valid benchmark to establish which of the two approaches is most suitable to describe the switching behavior of STT-MRAM devices.

In the presence of elongated FLs, the switching of the whole layer at the same time is not guaranteed and magnetization textures or domain walls can be formed during the magnetization reversal process. In this case, both Slonczewski and Zhang-Li torque contributions are present, and the proposed approach is able do deal with them on equal footing. In order to analyze how the MTJ presence affects the Zhang-Li (ZL) torque, we generalized the expression reported in [8] to include λ_φ:

$$\mathbf{T_{ZL}} = -\frac{\mu_B}{e} \frac{\beta_\sigma}{1+(\epsilon+\epsilon')^2} \left(\left(1 + \epsilon' \left(\epsilon + \epsilon'\right)\right) \mathbf{m} \times \right.$$
$$\left. \left[\mathbf{m} \times \left(\mathbf{J_C} \cdot \nabla\right) \mathbf{m}\right] - \epsilon\, \mathbf{m} \times \left(\mathbf{J_C} \cdot \nabla\right) \mathbf{m}\right) \tag{6}$$

$\epsilon = \left(\lambda_J/\lambda_{sf}\right)^2$ and $\epsilon' = \left(\lambda_J/\lambda_\varphi\right)^2$. We computed the torque in a structure with elongated RL and FL of 5 nm and 15 nm thickness, respectively, separated by a TB 0.9 nm thick. The magnetization of the RL is uniform along the x direction, while the FL presents a textured magnetization going from the z to the -x direction. The torque is computed assuming fast absorption of the transverse components, and is reported in Fig. 5. Fig. 5(a) shows how both the Slonczewski contribution near the TB interface, and the ZL contribution in the bulk of the layer are present. In Fig. 5(b), the ZL contribution is compared to the one obtained by applying (6) to the magnetization configuration of the FL, using the same values for λ_J, λ_φ, λ_{sf}, β_σ, and $\mathbf{J_C}$ employed for the spin drift-diffusion solution. The comparison reveals a substantial difference. The reason for this discrepancy lies in the fact that the presence of the TB also generates a weakly decaying spin accumulation component parallel to the magnetization, whose interaction with the magnetization texture substantially modifies the Zhang-Li contribution. The extended spin drift-diffusion approach thus allows to capture interdependent effects in the presence of both MTJs and domain walls or magnetization textures in the ferromagnetic layers.

4. Conclusion

We presented an extension of the drift-diffusion formalism capable of reproducing properties of the torque in magnetic tunnel junctions. We showed how the model can be further augmented to include ballistic corrections to the spin current and generate a more complex thickness dependence of the average torque compared to the one obtained with interfacial absorption. Our modeling approach clearly demonstrates that in the presence of an MTJ the Slonczewski and Zhang-Li contributions are not independent, and that a unified treatment of the torque is needed in order to accurately describe the switching process in ultra-scaled MRAM cells with elongated and composite ferromagnetic layers.

Declaration of competing interest

The authors declare that they have no known competing financial interests or personal relationships that could have appeared to influence the work reported in this paper.

Data availability

Data will be made available on request.

Acknowledgments

The financial support by the Austrian Federal Ministry for Digital and Economic Affair, Austria, the National Foundation for Research, Technology and Development, Austria and the Christian Doppler Research Association, Austria is gratefully acknowledged.

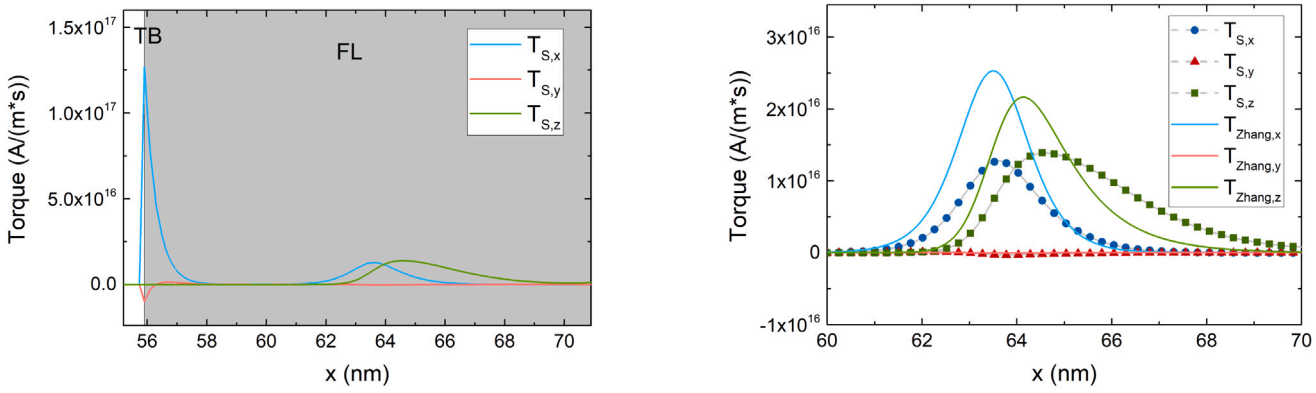

(a) (b)

Fig. 5. (a) Spin torque in an elongated FL with the magnetization going from z to -x. The magnetization in the RL is along x. (b) Comparison of the spin torque to the Zhang Li expression.

References

[1] Aggarwal S, Almasi H, DeHerrera M, Hughes B, Ikegawa S, Janesky J, et al. Demonstration of a reliable 1 Gb standalone spin-transfer Torque MRAM for industrial applications. In: Proc. IEDM conf.. 2019, p. 2.1.1–4. http://dx.doi.org/10.1109/IEDM19573.2019.8993516.

[2] Alzate JG, Arslan U, Bai P, Brockman J, Chen YJ, Das N, et al. 2 MB array-level demonstration of STT-MRAM process and performance towards L4 cache applications. In: Proc. IEDM conf.. 2019, p. 2.4.1–4. http://dx.doi.org/10.1109/IEDM19573.2019.8993474.

[3] Naik VB, Yamane K, Lee T, Kwon J, Chao R, Lim J, et al. JEDEC-qualified highly reliable 22nm FD-SOI embedded MRAM for low-power industrial-grade, and extended performance towards automotive-grade-1 applications. In: Proc. IEDM conf.. 2020, p. 11.3.1–4. http://dx.doi.org/10.1109/IEDM13553.2020.9371935.

[4] Shih Y-C, Lee C-F, Chang Y-A, Lee P-H, Lin H-J, Chen Y-L, et al. A reflow-capable, embedded 8Mb STT-MRAM macro with 9ns read access time in 16nm FinFET logic CMOS process. In: Proc. IEDM conf.. 2020, p. 11.4.1–4. http://dx.doi.org/10.1109/IEDM13553.2020.9372115.

[5] Han SH, Lee JM, Shin HM, Lee JH, Suh KS, Nam KT, et al. 28 Nm 0.08 mm^2/Mb embedded MRAM for frame buffer memory. In: Proc. IEDM conf.. 2020, p. 11.2.1–4. http://dx.doi.org/10.1109/IEDM13553.2020.9372040.

[6] Slonczewski JC. Currents, torques, and polarization factors in magnetic tunnel junctions. Phys Rev B 2005;71:024411. http://dx.doi.org/10.1103/PhysRevB.71.024411.

[7] Jinnai B, Igarashi J, Watanabe K, Funatsu T, Sato H, Fukami S, et al. High-performance shape-anisotropy magnetic tunnel junctions down to 2.3 nm. In: Proc. IEDM conf.. 2020, p. 24.6.1–4. http://dx.doi.org/10.1109/IEDM13553.2020.9371972.

[8] Zhang S, Li Z. Roles of nonequilibrium conduction electrons on the magnetization dynamics of ferromagnets. Phys Rev Lett 2004;93:127204. http://dx.doi.org/10.1103/PhysRevLett.93.127204.

[9] Abert C, Ruggeri M, Bruckner F, Vogler C, Hrkac G, Praetorius D, et al. A three-dimensional spin-diffusion model for micromagnetics. Sci Rep 2015;5(1):14855. http://dx.doi.org/10.1038/srep14855.

[10] Lepadatu S. Unified treatment of spin torques using a coupled magnetisation dynamics and three-dimensional spin current solver. Sci Rep 2017;7(1):12937. http://dx.doi.org/10.1038/s41598-017-13181-x.

[11] Fiorentini S, Ender J, Selberherr S, de Orio R, Goes W, Sverdlov V. Coupled spin and charge drift-diffusion approach applied to magnetic tunnel junctions. Sol -St El 2021;186:108103. http://dx.doi.org/10.1016/j.sse.2021.108103.

[12] Chshiev M, Manchon A, Kalitsov A, Ryzhanova N, Vedyayev A, Strelkov N, et al. Analytical description of ballistic spin currents and torques in magnetic tunnel junctions. Phys Rev B 2015;92:104422. http://dx.doi.org/10.1103/PhysRevB.92.104422.

[13] Camsari KY, Ganguly S, Datta D, Datta S. Physics-based factorization of magnetic tunnel junctions for modeling and circuit simulation. In: Proc. IEDM conf.. 2014, p. 35.6.1–4. http://dx.doi.org/10.1109/IEDM.2014.7047177.

[14] Brataas A, Bauer GE, Kelly PJ. Non-collinear magnetoelectronics. Phys Rep 2006;427(4):157–255. http://dx.doi.org/10.1016/j.physrep.2006.01.001.

[15] Graczyk P, Krawczyk M. Nonresonant amplification of spin waves through interface magnetoelectric effect and spin-transfer torque. Sci Rep 2021;11(1):15692. http://dx.doi.org/10.1038/s41598-021-95267-1.

[16] Petitjean C, Luc D, Waintal X. Unified drift-diffusion theory for transverse spin currents in spin valves, domain walls, and other textured magnets. Phys Rev Lett 2012;109:117204. http://dx.doi.org/10.1103/PhysRevLett.109.117204.